

Counterfactual Learning of Continuous Stochastic Policies

Houssam Zenati^{1,2}, Alberto Bietti³, Matthieu Martin¹, Eustache Diemert¹, and
Julien Mairal²

¹Criteo AI Lab

²Univ. Grenoble Alpes, Inria, CNRS, Grenoble INP, LJK, 38000 Grenoble, France

³Center for Data Science, New York University. New York, USA

Abstract

Counterfactual reasoning from logged data has become increasingly important for many applications such as web advertising or healthcare. In this paper, we address the problem of counterfactual risk minimization (CRM) for learning a stochastic policy with continuous actions. First, we introduce a new modelling strategy based on a joint kernel embedding of contexts and actions, which overcomes the shortcomings of previous discretization strategies. Second, we empirically show that the optimization perspective of CRM is more important than previously thought, and we demonstrate the benefits of proximal point algorithms and differentiable estimators. Finally, we propose an evaluation protocol for offline policies in real-world logged systems, which is challenging since policies cannot be replayed on test data, and we release a new large-scale dataset along with multiple synthetic, yet realistic, evaluation setups.¹

1 Introduction

Logged interaction data is widely available in many applications such as drug dosage prescription [17], recommender systems [21], or online auctions [8]. An important task is then to leverage past data in order to find a good *policy* for selecting actions (*e.g.*, drug doses) from available features (or *contexts*), rather than relying on randomized trials or sequential exploration, which may be costly or even sometimes unethical.

More precisely, we consider offline logged bandit feedback data, consisting of contexts, actions selected by a given *logging policy*, associated to observed rewards. This is known as *bandit feedback*, since the reward is only observed for the action chosen by the logging policy. The problem of finding a good policy thus requires a form of *counterfactual* reasoning to estimate what the rewards would have been, had we used a different policy. When the logging policy is stochastic, one may obtain unbiased reward estimates under a new policy through importance sampling with inverse propensity scoring [IPS, 13]. One may then use this estimator or its variants for optimizing new policies without the need for costly experiments [8, 10, 32, 33], an approach also known as counterfactual risk minimization (CRM). While this setting is not sequential, we assume that learning a *stochastic* policy is required so that one may gather new exploration data after deployment.

In this paper, we focus on stochastic policies with continuous actions, which, unlike the discrete setting, have received little attention in the context of counterfactual policy optimization [9, 17]. As noted by Kallus and Zhou [17] and as our experiments confirm, addressing the continuous case with naive discretization strategies performs poorly. Our first contribution is to introduce a joint nonlinear embedding of continuous actions and contexts relying on kernel methods, which yields competitive results with the state of the art.

In our second contribution, we underline the role of optimization algorithms for solving non-convex CRM problems [8, 33]. We believe that this aspect was overlooked, as previous work has mostly studied the

¹The code with open-source implementations for experimental reproducibility is available at <https://github.com/criteo-research/optimization-continuous-action-crm>.

effectiveness of *estimation* methods regardless of the optimization procedure. In this paper, we show that appropriate tools can bring significant benefits. To that effect, we introduce differentiable estimators based on soft-clipping the importance weights, which are more amenable to gradient-based optimization than previous hard clipping procedures [8, 34]. We also find that proximal point algorithms [28] tend to dominate simpler off-the-shelf optimization approaches.

Finally, we propose a new offline evaluation benchmark for logged data with continuous actions by releasing a large-scale dataset of logged exploration data from a real-world system with more than 100 million samples, and a protocol for estimating test performance in an off-policy manner.

This protocol relies on importance sampling diagnostics to discard unreliable solutions and significance tests to assess improvements to a reference policy.

We believe that our dataset release together with this evaluation protocol will be useful for the research community, as counterfactual optimization of continuous-action policies with real-life data is a challenging and important problem, which raises many difficulties that remain to be solved.

2 Related Work

A large effort has been devoted to designing CRM estimators that have less variance than the IPS method, through clipping importance weights [8, 34], variance regularization [32], or by leveraging reward estimators through doubly robust methods [10, 27]. In order to tackle an overfitting phenomenon termed “propensity overfitting”, Swaminathan and Joachims [33] also consider self-normalized estimators [25]. Such estimation techniques also appear in the context of sequential learning in contextual bandits, where the goal of the agent is to find a good policy in a sequential manner while minimizing regret [2, 19], as well as for off-policy evaluation in reinforcement learning [14]. In contrast, the setting considered in our work is not sequential.

While most approaches for counterfactual policy optimization tend to focus on discrete actions, few works have tackled the continuous action case, again with a focus on estimation rather than optimization. In particular, propensity scores for continuous actions were considered first by Hirano and Imbens [12]. More recently, evaluation and optimization of continuous action policies were studied in a non-parametric context by [17] using kernel smoothing, and by [9] in a semi-parametric setting.

In contrast to these previous methods, (i) we focus on stochastic policies while they consider deterministic ones,

since we are interested in generating randomized data for future offline experiments. (ii) The terminology of *kernels* used by Kallus and Zhou [17] refers to a different mathematical tool than the kernel embedding used in our work. We use positive definite kernels to define a nonlinear representation of actions and contexts in order to model the reward function, whereas Kallus and Zhou [17] use *kernel density estimation* to obtain good importance sampling estimates. We note that Krause and Ong [18] use similar kernels to ours for jointly modeling contexts and actions, but in the different setting of sequential decision making with upper confidence bound strategies. (iii) While Kallus and Zhou [17] focus on *estimation* with linear policies, our work focuses on the questions of *representation* and *optimization*: in particular, we introduce a new contextual policy parameterization, which leads to significant gains compared to linear policies on the problems we consider, as well as further improvements related to the optimization strategy.

Optimization methods for learning stochastic policies have been mainly studied in the context of reinforcement learning through the policy gradient theorem [3, 31, 36]. Such methods typically need to observe samples from the new policy at each optimization step, which is not possible in our off-policy setting. Other methods leverage a form of off-policy estimates during optimization for improving the policy at each step [16, 29], but this still requires fresh samples, while we consider objective functions involving only a fixed dataset of collected data. In the context of CRM, [30] introduce an estimator with a continuous clipping objective that achieves an improved bias-variance trade-off over the doubly-robust strategy. Nevertheless, this estimator is non-smooth, unlike our soft-clipping estimator.

3 Contextual and Continuous Actions Modeling for CRM

We now review the *counterfactual risk minimization* framework, and then present new modelling approaches for stochastic policies with continuous actions.

3.1 Background

For a stochastic policy π over a set of actions \mathcal{A} , a contextual bandit environment generates i.i.d. context features $x \sim \mathcal{D}_X$ in \mathcal{X} , actions $a \sim \pi(\cdot|x)$ and feedbacks/losses $y \sim D_Y(\cdot|x, a)$ with expectation $\mathbb{E}[y|x, a] = \eta^*(x, a)$. We denote the resulting distribution over triplets (x, a, y) as \mathcal{D}_π . We consider a logged dataset (x_i, a_i, y_i) , $i = 1, \dots, n$, where we assume $(x_i, a_i, y_i) \sim \mathcal{D}_{\pi_0}$ i.i.d. for a given stochastic logging policy π_0 , and we assume the propensities $\pi_{0,i} := \pi_0(a_i|x_i)$ to be known. In the continuous action case, probabilities are *densities* thus propensities denote the density function of π_0 evaluated on the actions. The expected loss or risk of a policy π is then given by

$$L(\pi) = \mathbb{E}_{(x,a,y) \sim \mathcal{D}_\pi} [y]. \quad (1)$$

For the logged bandit, the task is to determine a policy $\hat{\pi}$ in a set of *stochastic* policies Π with small risk. Note that this definition may also include deterministic policies by allowing Dirac masses (in fact, the minimizer of (1), given by $\pi^*(x) = \arg \min_a \eta^*(x, a)$, is deterministic), but it may be desirable to enforce a minimum variance in order to perform future offline experiments, assuming $\hat{\pi}$ is meant to be deployed. In our setting, the expectation in (1) cannot be computed directly for any π , as the available interaction data comes from a different distribution \mathcal{D}_{π_0} . Yet, multiple empirical estimators of the risk hereafter allow to derive an empirical optimal policy that is found by solving:

$$\hat{\pi} \in \arg \min_{\pi \in \Pi} \hat{L}(\pi) + \Omega(\pi), \quad (2)$$

where the objective consists of an empirical estimate \hat{L} of the risk and of possible data-dependent regularizers, denoted by Ω . When using counterfactual estimators for \hat{L} , this method has been called *counterfactual risk minimization* [32].

The counterfactual approach tackles the distribution mismatch between the logging policy $\pi_0(\cdot|x)$ and a policy π in Π via importance sampling. The IPS method [13] relies on correcting the distribution mismatch using the relation

$$L(\pi) = \mathbb{E}_{(x,a,y) \sim \mathcal{D}_{\pi_0}} \left[y \frac{\pi(a|x)}{\pi_0(a|x)} \right], \quad (3)$$

assuming π_0 has non-zero mass on the support of π , which allows us to derive an unbiased empirical estimate

$$\hat{L}_{\text{IPS}}(\pi) = \frac{1}{n} \sum_{i=1}^n y_i \frac{\pi(a_i|x_i)}{\pi_{0,i}}. \quad (4)$$

Since the empirical estimator $\hat{L}_{\text{IPS}}(\pi)$ has large variance and is subject to various overfitting phenomena, regularization strategies have been proposed, such as clipping the importance sampling (cIPS) weights [8], or the *self-normalized* (SNIPS) estimator [33], see Appendix 8 for a review of these estimators.

Another approach is to directly fit the loss values in observed data with a direct estimator $\hat{\eta}(x, a)$, for instance by using ridge regression to fit $y_i \approx \hat{\eta}(x_i, a_i)$, and then to use the deterministic greedy policy $\hat{\pi}(x) = \arg \min_a \hat{\eta}(x, a)$. This approach, termed direct method (DM), has the benefit of avoiding the high-variance problems of IPS-based methods, but may suffer from large bias since it ignores the potential mismatch between $\hat{\pi}$ and π_0 . Specifically, the bias is problematic when the logging policy provides unbalanced data samples (*e.g.*, samples actions in a specific area only) leading to overfitting [8, 10, 33]. Conversely, counterfactual methods re-balance these generated data samples with importance weights and mitigate the distribution mismatch of the samples to better estimate reward function on unexplored actions. Nevertheless, such loss estimators can be effective when few samples are available, and may be combined with IPS estimators (see Appendix 8) in the so-called doubly robust (DR) estimator [10].

3.2 New Parameterization for Stochastic Policies on Continuous Actions

When considering continuous action spaces, the choice of policies is more involved than in the discrete case. While one may discretize the action space into buckets and leverage discrete action strategies, but (i) local information within each bucket is lost, (ii) the discretization does not take into account the structure of the action space, and (iii) the policies obtained by predicting a finite set of actions become discontinuous. Besides, in order to have unbiased estimators, the logged propensities $\pi_{0,i}$ need to be tailored to the specific discretization, which may be impractical since it depends on the choice of buckets.

In this paper, we thus focus on stochastic policies belonging to certain classes of continuous distributions, such as normal or log-normal. Specifically, we consider a set of context-dependent policies $\Pi = \{\pi_\theta, \theta \in \Theta\}$ parameterized by $\theta = (\mu(x), \sigma)$, with mean $\mu(x)$ and standard deviation σ such as $\pi_\theta(\cdot|x) = \mathcal{N}(\mu(x), \sigma^2)$. As a simple baseline, one may take $\mu(x) = \mu^\top \varphi(x)$, where $\varphi(x)$ could be a piecewise constant, linear, or non-linear representation of x . While such baselines can be effective in simple problems, they may be limited in more difficult scenarios where the expected loss has a complex behavior as a function of a , *e.g.*, multiple modes. This motivates the need for classes of policies which can better capture such variability by considering a joint model $\eta(x, a)$ of the loss/reward.

The counterfactual loss predictor (CLP). Given such a model $\eta(x, a)$, which we call *loss predictor*, we parametrize the mean of a stochastic policy by using a soft-argmax operator with temperature γ :

$$\mu_{\text{CLP}}(x) = \sum_{i=1}^m a_i \frac{\exp(-\gamma\eta(x, a_i))}{\sum_{j=1}^m \exp(-\gamma\eta(x, a_j))}, \quad (5)$$

where a_1, \dots, a_m are anchor points (*e.g.*, a regular grid or quantiles of the action space), and μ_{CLP} may be viewed as a smooth approximation of a greedy policy $\mu_{\text{greedy}}(x) = \arg \min_a \eta(x, a)$. Our estimator allows using η from a rich class of context-action models, while avoiding the need for optimization over actions, and making the resulting CRM problem differentiable.

Loss predictors based on kernels. The above CLP model is parameterized by regressors $\eta(x, a)$ that may be interpreted as loss predictors. In a continuous action problem, a reasonable assumption is that losses vary smoothly as a function of actions. Then, a good choice is to take η in a space of smooth functions such as the reproducing kernel Hilbert space \mathcal{H} (RKHS) defined by a positive definite kernel [*e.g.*, ?], so that one may control the smoothness of η through regularization with the RKHS norm. More precisely, we consider kernels of the form $K((x, a), (x', a')) = K_{\mathcal{X}}(x, x')K_{\mathcal{A}}(a, a')$, which correspond to a tensor product feature map $\varphi(x, a) = \varphi_{\mathcal{X}}(x) \otimes \varphi_{\mathcal{A}}(a)$. For simplicity, we consider linear or quadratic kernels on contexts, leading to $\varphi_{\mathcal{X}}(x) = x$ or $\varphi_{\mathcal{X}}(x) = (xx^T, x)$, noting that more complex kernels may also be used. For actions, however, it is important to use a richer kernel such as the Gaussian kernel, which allows us to approximate complex feedback functions.

Nyström approximation. For computational efficiency, we rely on a Nyström approximation [35] of $\varphi_{\mathcal{A}}$ instead of using the exact kernel, which amounts to replacing $\varphi_{\mathcal{A}}$ by its projection on a finite-dimensional subspace of the RKHS $\mathcal{F} = \text{span}\{(\varphi_{\mathcal{A}}(\bar{a}_1), \dots, \varphi_{\mathcal{A}}(\bar{a}_m))\}$ for a set of anchor points $\bar{A} = \{\bar{a}_1, \dots, \bar{a}_m\}$. In practice, we may choose \bar{a}_i to be equal to the a_i in (5). The Nyström approximation then considers the embedding $\psi_{\mathcal{A}}(a) = K_{AA}^{-1/2}K_A(a)$, where $K_{AA} = [K_{\mathcal{A}}(\bar{a}_i, \bar{a}_j)]_{ij}$ and $K_A(a) = [K_{\mathcal{A}}(a, \bar{a}_i)]_i$, and we consider models of the form

$$\eta_{\text{CLP}}(x, a) = \langle \beta_{\text{CLP}}, \varphi_{\mathcal{X}}(x) \otimes \psi_{\mathcal{A}}(a) \rangle,$$

where ℓ^2 regularization on β corresponds to controlling the RKHS norm and the smoothness of η . In practice, we learn parameters $\theta = (\beta_{\text{CLP}}, \sigma)$, where σ^2 is the variance of the stochastic policy. Moreover, even with a small number of anchor points, we may obtain a good approximation of the full kernel method, particularly when losses vary smoothly with actions, while other strategies based on discretizing the action space may require a much finer discretization, and tend to be less robust to this choice, as verified in our experiments (see Section 6). The model is illustrated in Figure 1.

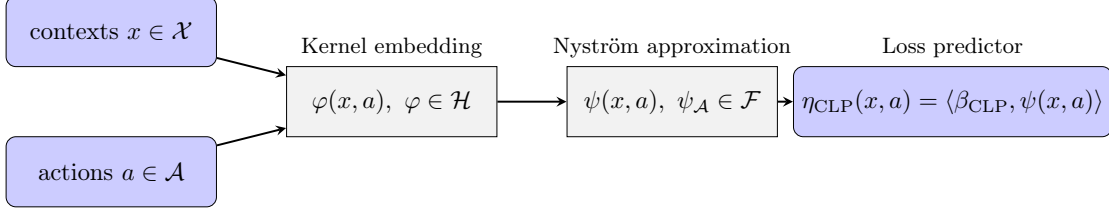


Figure 1: **Joint kernel embedding for the counterfactual loss predictor (CLP)**. η_{CLP} uses a kernel embedding with Nyström approximation for the parametrization of the stochastic policy.

4 Optimization for CRM

We now present optimization aspects of the CRM problem, as well as a new differentiable estimator.

Soft Clipping IPS. The hard clipping estimator $\hat{L}_{\text{clIPS}}^M(\pi) = \frac{1}{n} \sum_{i=1}^n y_i \min\{\pi(a_i|x_i)/\pi_{0,i}, M\}$ makes the objective function non-differentiable, and also causes terms in the objective with clipped weights to have vanishing gradient. In other words, a trivial stationary point of the objective function is that of a stochastic policy that differs enough from the logging policy such that all importance weights are clipped. To alleviate this issue, we propose a differentiable logarithmic soft-clipping strategy. Given a threshold parameter $M \geq 0$ and an importance weight $w_i = \pi(a_i|x_i)/\pi_{0,i}$, we consider the soft-clipped weights:

$$\zeta(w_i, M) = \begin{cases} w_i & \text{if } w_i \leq M \\ \alpha(M) \log(w_i + \alpha(M) - M) & \text{otherwise,} \end{cases} \quad (6)$$

where $\alpha(M)$ is such that $\alpha(M) \log(\alpha(M)) = M$, which yields a differentiable operator. We give further explanations about the benefits of clipping strategies as well as an illustration of this estimator in Appendix 9.2. Then, the IPS estimator with soft clipping becomes

$$\hat{L}_{\text{scIPS}}^M(\pi) = \frac{1}{n} \sum_{i=1}^n y_i \zeta\left(\frac{\pi(a_i|x_i)}{\pi_{0,i}}, M\right). \quad (7)$$

In Appendix 13, we prove that the variance-regularized version of this estimator enjoys a similar generalization bound to that of Swaminathan and Joachims [32] for the hard-clipped version, and hence provides a good optimization objective for minimizing the expected risk.

Proposition 4.1 (Generalization bound for \hat{R}_{scIPS}^M). *Assume losses y_i in $[-1, 0]$ and importance weights bounded by W . With probability $1 - \delta$, for all π in Π ,*

$$L(\pi) \leq \hat{L}_{\text{scIPS}}^M(\pi) + O\left(\sqrt{\frac{\hat{V}(\pi)C_n(\Pi, \delta)}{n}} + \frac{SC_n(\Pi, \delta)}{n}\right),$$

where $S = \zeta(W, M) = O(\log W)$, \hat{V} denotes the empirical variance of the loss estimates, and $C_n(\Pi, \delta)$ is a complexity measure of the policy class (see Appendix 13).

Note that the result requires bounded importance weights in contrast to hard-clipping, which is not a problem in practice when using bounded actions (e.g., due to system constraints) and a π_0 with a non-zero lower bound on this bounded support. Moreover, the dependence on W is only logarithmic compared to a linear dependence for IPS, and we gain significant benefits in terms of optimization by having a smooth objective.

Proximal Point Algorithms. Non-convex CRM objectives have been optimized with classical gradient-based methods [32, 33] such as L-BFGS [22], or the stochastic gradient descent approach [15, 32].

Proximal point methods are classical approaches originally designed for convex optimization [28], which were then found to be useful for nonconvex functions [11, 26]. In order to minimize a function \mathcal{L} , the main idea is to approximately solve a sequence of subproblems that are better conditioned than \mathcal{L} , such that the sequence of iterates converges towards a better stationary point of \mathcal{L} . More precisely, the proximal point method consists of computing a sequence

$$\theta_k \approx \arg \min_{\theta} \left(\mathcal{L}(\theta) + \frac{\kappa}{2} \|\theta - \theta_{k-1}\|_2^2 \right), \quad (8)$$

where $\mathcal{L}(\theta) = \hat{L}(\pi_\theta) + \Omega(\pi_\theta)$ and $\kappa > 0$ is a constant parameter. By regularizing the loss with a quadratic function, the subproblems become intuitively “less nonconvex” and for many machine learning formulations, it is even possible to obtain convex sub-problems with large enough κ [see 26]. In this paper, we will consider such a strategy (8) with a parameter κ , which we set to zero only for the last iteration.

Note that the effect of the proximal point algorithm differs from the proximal policy optimization (PPO) strategy used in reinforcement learning [29], even though both approaches are related. PPO encourages a new stochastic policy to be close to a previous one in Kullback-Leibler distance. Whereas the term used in PPO modifies the objective function (and changes the set of stationary points), the proximal point algorithm optimizes and finds a stationary point of the original objective \mathcal{L} (even with fixed $\kappa > 0$).

5 A new Dataset and Evaluation Benchmark

Evaluating new policies for real systems is challenging as it is often undesirable or even impossible to roll-out policy candidates. It is thus important to have reliable offline evaluation methods from logged data. In the continuous action domain, previous work have mainly considered semi-simulated scenarios [6, 17], where contexts are taken from supervised datasets but rewards are synthetically generated. To foster research on practical continuous policy optimization we release a new, large scale dataset called CoCoA, which to our knowledge is the first to provide logged exploration data from a real-world system with continuous actions. Additionally, we introduce a benchmark protocol for properly evaluating continuous policies on this dataset using off-policy evaluation.

5.1 The CoCoA Dataset

The CoCoA dataset comes from the Criteo digital advertising company that ran an experiment involving a randomized, continuous policy for real-time bidding. Data has been properly anonymized so as to not disclose any private information. Each sample represents a bidding opportunity for which a multi-dimensional context x in \mathbb{R}^d is observed and a continuous action a in \mathbb{R}^+ has been chosen according to a stochastic policy π_0 that is logged along with the reward $-y$ (meaning loss y) in \mathbb{R} . The reward represents an advertising objective such as sales or visits and is jointly caused by the action and context (a, x) . Particular care has been taken to guarantee that each sample $(x_i, a_i, \pi_0(a_i|x_i), y_i)$ is independent. The goal is to learn a contextual, continuous, stochastic policy $\pi(a|x)$ that generates more reward in expectation than π_0 , evaluated offline, while keeping some exploration (stochastic part). As can be observed in Table 1, a typical feature of this dataset is the high variance of the reward, motivating the scale of the dataset to obtain precise counterfactual estimates. The link to download the dataset is available in the code repository: <https://github.com/criteo-research/optimization-continuous-action-crm>.

Table 1: **CoCoA dataset** summary statistics.

N	d	$\mathbb{E}[-Y]$	$\mathbb{V}[Y]$	$\mathbb{V}[A]$	$\mathbb{P}(Y \neq 0)$
120.10 ⁶	3	11.37	9455	.01	.07

5.2 Evaluation Benchmark for Logged Data

In order to estimate the test performance of a policy on our CoCoA dataset, off-policy evaluation is needed, as we only have access to logged exploration data. Yet, this involves in practice a number of choices and difficulties, the most documented being i) potentially infinite variance of IPS estimators [8] and ii) propensity over-fitting [32, 33]. The former implies that it can be difficult to accurately assess the performance of new policies due to large confidence intervals, while the latter may lead to estimates that reflect large importance weights rather than rewards. A proper evaluation protocol should therefore guard against such outcomes.

A first, structuring choice is the IPS estimator. While variants of IPS exist to reduce variance, such as clipped IPS, we found self-normalized IPS [SNIPS, 33, 20, 25, 24] to be more effective in practice. Indeed, it avoids the choice of a clipping threshold, generally reduces variance and is equivariant with respect to translation of the reward.

A second component is the use of importance sampling diagnostics to prevent propensity over-fitting. [20] propose to check if the empirical average of importance weights deviates from 1. However, there is no precise guideline based on this quantity to reject estimates. Instead, we recommend to use a diagnostic on the *effective sample size* $n_{\text{eff}} = (\sum_{i=1}^n w_i)^2 / \sum_{i=1}^n w_i^2$, which measures how many samples are actually usable to perform estimation of the counterfactual estimate; we follow [25], who recommends to reject the estimate when the relative effective sample size n_{eff}/n is less than 1%.

A third choice is a statistical decision procedure to check if $L(\pi) < L(\pi_0)$. In theory, any statistical test against a null hypothesis $H_0: L(\pi) \geq L(\pi_0)$ with confidence level $1 - \delta$ can be used.

Finally, it is difficult to design an appropriate protocol that controls variance, propensity over-fitting and statistical robustness of the estimate. As a first step in that direction, we propose Algorithm 1 that summarizes our protocol design.

Since we may not evaluate such a protocol on purely offline data, we performed an empirical evaluation on synthetic setups where we could analytically design true positive ($L(\pi) < L(\pi_0)$) and true negative policies. We discuss subsequently in Sec. 6 the concrete parameters of Alg. 1 and their influence on false (non-)discovery rates in practice.

Algorithm 1 Benchmark Evaluation Protocol v1

- Input:** $1 - \delta$: confidence of statistical test (def: 0.95); ν : a max deviance ratio (def: 0.01);
Output: counter-factual estimation of $L(\pi)$ and decision to reject the null hypothesis $H_0: L(\pi) \geq L(\pi_0)$.
1. Split dataset $\mathcal{D} \mapsto \mathcal{D}^{\text{train}}, \mathcal{D}^{\text{valid}}, \mathcal{D}^{\text{test}}$
 2. Train new policy π on $\mathcal{D}^{\text{train}}$ while tuning hyper-parameters on $\mathcal{D}^{\text{valid}}$
 3. Estimate effective sample size $n_{\text{eff}}(\pi)$ on $\mathcal{D}^{\text{valid}}$
 4. Estimate $\hat{L}_{\text{SNIPS}}(\pi)$ on $\mathcal{D}^{\text{test}}$
- Return** if $\frac{n_{\text{eff}}}{n} > \nu$ (else “invalid”)
1. counterfactual estimator $\hat{L}_{\text{SNIPS}}(\pi)$;
 2. decide if $\hat{L}_{\text{SNIPS}}(\pi) < \hat{L}(\pi_0)$ on $\mathcal{D}^{\text{test}}$ with confidence $1 - \delta$.
-

6 Experimental Setup and Evaluation

We now introduce synthetic datasets that allow evaluation for any test policy; then, we present empirical findings on both these datasets and the CoCoA dataset.

6.1 Empirical Settings

Synthetic potential prediction. We introduce simple synthetic environments with the following generative process: an unobserved random group index g in \mathcal{G} is drawn, which influences the drawing of a context x and of an unobserved “potential” p in \mathbb{R} , according to a joint conditional distribution $P_{X,P|G}$. The observed reward $-y$ is then a function of the context x , action a , and potential p . The causal graph corresponding to

this process is given in Figure 2. Then, we generate three synthetic datasets (“noisymoos, noisycircles, and anisotropic”, abbreviated respect. “moos, circles, and GMM” in Table 2 and illustrated in Appendix 11.1, Figure 15), with two-dimensional contexts on 2 or 3 groups and different choices of $P_{X,P|G}$.

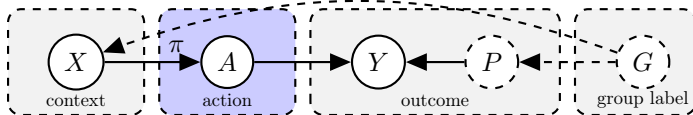


Figure 2: **Causal Graph of the synthetic setting.** A denotes the action, X the feature context, G the unobserved group label, Y the outcome and P the unobserved potential. Unobserved elements are dotted.

The goal is then to find a policy $\pi(a|x)$ that maximizes reward by adapting to the unobserved potential. For our experiments, potentials are normally distributed conditionally on the group index, $p|g \sim \mathcal{N}(\mu_g, \sigma^2)$. As many real-world applications feature a reward function that increases first with the action up to a peak and finally drops, we have chosen a piecewise linear function peaked at $a = p$ (see Appendix 11.1, Figure 16), that mimics overall reward buckets over the CoCoA dataset presented in Section 5. In bidding applications, the potential may represent an unknown true value for an advertisement, and the reward is then maximized when the bid (the action) matches this value. In medicine, increasing drug dosage may increase treatment effectiveness but threshold effects soon appear and if dosage is pushed further, secondary effects may eclipse benefits [4].

Semi-synthetic setting with medical data. We follow the setup of Kallus and Zhou [17] using a dataset on dosage of the Warfarin blood thinner drug [1]. The dataset consists of covariates about patients along with a dosage treatment prescription by a medical expert, which is a scalar value and thus makes the setting useful for continuous action modelling. While the dataset is supervised, we simulate a contextual bandit environment by using a hand-crafted reward function that is maximal for actions a that are within 10% of the expert’s therapeutic drug dosage, following Kallus and Zhou [17], see Appendix 11.1.

Evaluation methodology. In order to make our evaluation realistic, we always perform hyperparameter selection by using off-policy estimates on a validation set with propensities obtained from the same logging policy as the training set, even for synthetic datasets. We also use the strategies outlined in Section 5 to discard policies that cannot be evaluated correctly on the validation set. The same strategy is used for test estimates on the CoCoA dataset, while more accurate online estimates are used for test rewards in synthetic scenarios. See Appendix 11.2 for more details.

6.2 Empirical Evaluation

We now present an empirical validation of our proposed offline evaluation protocol, then empirical evaluations of our proposed CLP policy parametrization and influence of optimization-related techniques.

Validation of the offline benchmark evaluation protocol. Our first experiment consists of verifying that Alg. 1 is able of accurately deciding if a candidate policy π is better than the logging policy π_0 on synthetic data. For that purpose, we propose to generate true positive policies ($L(\pi) < L(\pi_0)$) by sampling parameters around the analytical optimal policy in the synthetic setup of Section 6.1. Conversely, we find true negative policies by sampling parameters around those of the logging (hence $\pi \approx \pi_0$). As the setup is synthetic, it is then easy to replay the policies π and check that indeed they are better or worse than π_0 .

Our first result is that SNIPS estimates are highly correlated to the true (online) reward (average $\rho = .968$, 30% higher than IPS, see plots in Appendix 10.1). Then, we showed that with a proper choice of the ν and δ parameters, it is possible to control the False Discovery Rate (FDR) ($< 10^{-4}$) and False Non-Discovery Rate (FNDR) ($< 5.10^{-4}$) on the same setup. We observed that on simple synthetic setups the effective sample

size criterion $\nu = n_{\text{eff}}/n$ is seldom necessary for policies close to the logging policy ($\pi \approx \pi_0$). For policies which were not close to the logging policy we found that standard statistical significance testing at $1 - \delta$ level was by itself not enough to guarantee a low FDR which justified the use of ν . Adjusting the effective sample size can therefore influence the performance of the protocol (see Appendix 10.2.3 for detailed results, 10.3 for further illustrations of importance sampling diagnostics). Further experiments in this section on the synthetic and CoCoA datasets use this protocol with $\delta = 0.05, \nu = 0.01$ to decide significance.

Continuous action space requires more than naive discretization strategies. In Figure 3, we compare our continuous approaches to discretized strategies that bucketize the action space and consider stochastic discrete-action policies on the resulting buckets, using IPS, DM or DR estimators. First, by appropriately incorporating the continuous action structure, we can see that continuous modelings, especially our CLP approach, have much better performance than the discrete approach on the synthetic datasets (see also Appendix 12.1), across all choices considered for the number of anchor points/buckets. The improvement is larger when using a small number of anchor points, illustrating that even a small number is sufficient to achieve precise action selection with our proposed Nyström approximation. In contrast, the discrete strategies require a much finer grid, and are thus also more computationally costly. The plots also show that our (stochastic) direct method strategy, where we add a minimal amount of noise to the deterministic DM in order to pass the $n_{\text{eff}}/n > \nu$ validation criterion, has similar benefits in terms of robustness to anchor points, thanks to our proposed similar Nyström parameterization. Nevertheless, it is overall outperformed by CLP, highlighting a benefit of using counterfactual methods compared to a direct fit to observed rewards, which may suffer from large bias.

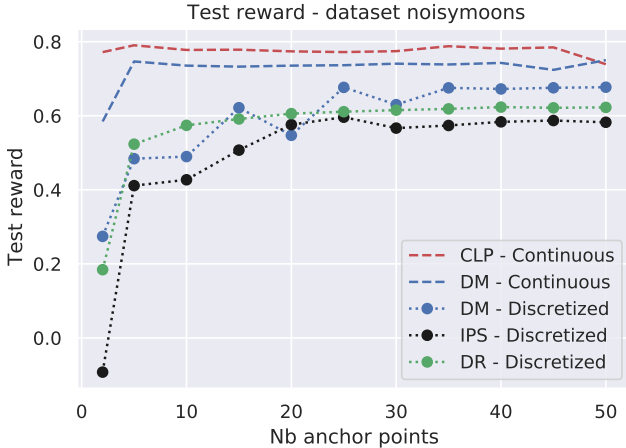


Figure 3: **Continuous vs discrete.** Test rewards with varying numbers of anchor points for our continuous proposed parametrization for CLP and DM, versus discrete approaches.

Counterfactual loss predictor (CLP) provides a competitive parameterization for continuous-action policy learning. Here we compare our CLP modelling approach to other baseline parameterized modelings (constant, linear and non-linear described in Section 3.2) on our synthetic and semi-synthetic setups described in Section 6.1 as well as our proposed real-world CoCoA dataset presented in Section 5.1. We also provide a baseline comparison to Kallus and Zhou [17], who propose a counterfactual method for learning *deterministic* policies with continuous actions, using kernel smoothing for density estimation. Their approach is based on optimal kernel bandwidth selection using a costly and approximate computation, which produced poor results in our setup; instead, we select the best bandwidth on a grid through cross-validation. We subsequently show in Table 2 a comparison of test rewards obtained with policies learned with the scIPS estimator (other estimators are shown in Appendix 12.2 in one standard deviation across-contexts for all datasets). Following Kallus and Zhou [17], we only consider the linear context parameterization baseline on

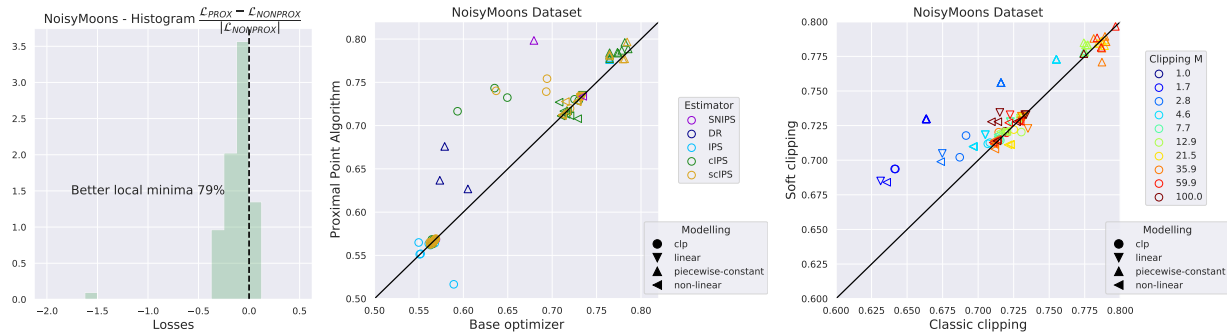


Figure 4: **Optimization-driven approaches.** Relative improvements in the training objective from using the proximal point method (left), comparison of test rewards for proximal point vs the simpler gradient-based method (center), and for soft- vs hard-clipping (right).

the high-dimensional Warfarin dataset, which achieves a similar reward to that reported by Kallus and Zhou [17], although our estimators and model selection criteria are somewhat different. Overall, we find our new counterfactual loss predictor (CLP) parameterization to improve on all other choices of parameterizations and baselines on these datasets, which again highlights the effectiveness of the reward predictor at exploiting the continuous action structure.

Table 2: **Policy parameterizations performance on all datasets.** Test rewards (higher the better) for the scIPS estimator ($\pm\sigma$ on CoCoA and * means the decision $L(\pi) \leq L(\pi_0)$ by Algo. 1). KZ refers to Kallus and Zhou [17].

	Circles	Moons	GMM	Warfarin	CoCoA
Constant	0.612	0.612	0.603	-10.05	11.36 ± 0.13
Linear	0.611	0.733	0.764	-10.29	8.00 ± 0.72
Poly	0.696	0.728	0.745	-	8.78 ± 0.51
CLP	0.767	0.781	0.770	-9.98	$11.44 \pm 0.10^*$
KZ	0.612	0.657	0.603	-10.19	$11.38 \pm 0.04^*$

Optimization-driven approaches influence counterfactual policy learning performance. Figure 4 shows the improvements in test reward and in training objective of our optimization-driven strategies, namely the soft-clipping estimator and the use of the proximal point algorithm. Figure 4 (left) illustrates the benefits of the proximal point method when optimizing the (non-convex) CRM objective in a wide range of hyperparameter configurations, and Figure 4 (center) shows that in many cases this results in an improvement in test reward as well. Here, each point compares the test metric for fixed models as well as initialization seeds, while optimizing the remaining hyperparameters on the validation set. In Figure 4 (right), the points correspond to different choices of the clipping parameter M , models and initialization, with the rest of the hyper-parameters optimized on the validation set. This plot also shows that the smoothness of the objective in soft clipping compared to hard clipping provides benefits in terms of test reward, perhaps thanks to a more favorable optimization landscape. Overall, these figures confirm that the optimization perspective is an important one when considering CRM problems.

7 Conclusion and Future Work

In this work, we first propose a new contextual estimator with a joint kernel embedding of contexts and actions, showing superior empirical performance on a range of problems. Second, we underline the importance of

optimization in CRM formulations with a soft-clipping estimator and the use of proximal point methods. Third, we propose an offline evaluation protocol and a new large-scale dataset, which, to the best of our knowledge, is the first with real-world logged propensities and continuous actions. An interesting future direction would be to see the gains that may be achieved with multiple sequential rounds of offline counterfactual optimization.

Acknowledgments

The authors thank Christophe Renaudin (Criteo AI Lab) for his help in the data collection and engineering which was necessary for this project. JM was supported by the ERC grant number 714381 (SOLARIS project) and by ANR 3IA MIAI@Grenoble Alpes, (ANR-19-P3IA-0003). AB acknowledges support from the ERC grant number 724063 (SEQUOIA project).

References

- [1] Estimation of the Warfarin dose with clinical and pharmacogenetic data. *New England Journal of Medicine*, 360(8):753–764, 2009.
- [2] A. Agarwal, D. Hsu, S. Kale, J. Langford, L. Li, and R. Schapire. Taming the monster: A fast and simple algorithm for contextual bandits. In *International Conference on Machine Learning (ICML)*, 2014.
- [3] Z. Ahmed, N. Le Roux, M. Norouzi, and D. Schuurmans. Understanding the impact of entropy on policy optimization. In *International Conference on Machine Learning (ICML)*, 2019.
- [4] C. D. Barnes and L. G. Eltherington. *Drug dosage in laboratory animals: a handbook*. Univ of California Press, 1966.
- [5] Y. Benjamini and Y. Hochberg. Controlling the false discovery rate: A practical and powerful approach to multiple testing. *Journal of the Royal Statistical Society Series B (Methodological)*, 57(1):289–300, 1995. doi: <http://dx.doi.org/10.2307/2346101>. URL <http://dx.doi.org/10.2307/2346101>.
- [6] D. Bertsimas and C. McCord. Optimization over continuous and multi-dimensional decisions with observational data. In *Advances in Neural Information Processing Systems (NeurIPS)*, 2018.
- [7] C. Bonferroni. Teoria statistica delle classi e calcolo delle probabilita. *Pubblicazioni del R Istituto Superiore di Scienze Economiche e Commerciali di Firenze*, 8:3–62, 1936. URL <https://ci.nii.ac.jp/naid/20001561442/en/>.
- [8] L. Bottou, J. Peters, J. Quiñero Candela, D. X. Charles, D. M. Chickering, E. Portugaly, D. Ray, P. Simard, and E. Snelson. Counterfactual reasoning and learning systems: The example of computational advertising. *Journal of Machine Learning Research (JMLR)*, 14(1):3207–3260, Jan. 2013.
- [9] M. Demirer, V. Syrgkanis, G. Lewis, and V. Chernozhukov. Semi-parametric efficient policy learning with continuous actions. In *Advances in Neural Information Processing Systems (NeurIPS)*, 2019.
- [10] M. Dudik, J. Langford, and L. Li. Doubly robust policy evaluation and learning. In *International Conference on Machine Learning (ICML)*, 2011.
- [11] M. Fukushima and H. Mine. A generalized proximal point algorithm for certain non-convex minimization problems. *International Journal of Systems Science*, 12(8):989–1000, 1981.
- [12] K. Hirano and G. W. Imbens. The propensity score with continuous treatments. *Applied Bayesian modeling and causal inference from incomplete-data perspectives*, 226164:73–84, 2004.
- [13] D. G. Horvitz and D. J. Thompson. A generalization of sampling without replacement from a finite universe. *Journal of the American Statistical Association*, 47(260):663–685, 1952.

- [14] N. Jiang and L. Li. Doubly robust off-policy value evaluation for reinforcement learning. In *International Conference on Machine Learning (ICML)*, 2016.
- [15] T. Joachims, A. Swaminathan, and M. de Rijke. Deep learning with logged bandit feedback. In *International Conference on Learning Representations (ICLR)*, 2018.
- [16] S. Kakade and J. Langford. Approximately optimal approximate reinforcement learning. In *International Conference on Machine Learning (ICML)*, 2002.
- [17] N. Kallus and A. Zhou. Policy evaluation and optimization with continuous treatments. In *International Conference on Artificial Intelligence and Statistics (AISTATS)*, 2018.
- [18] A. Krause and C. S. Ong. Contextual gaussian process bandit optimization. In *Advances in neural information processing systems (NIPS)*, pages 2447–2455, 2011.
- [19] J. Langford and T. Zhang. The epoch-greedy algorithm for multi-armed bandits with side information. In *Advances in Neural Information Processing Systems (NIPS)*, 2008.
- [20] D. Lefortier, A. Swaminathan, X. Gu, T. Joachims, and M. de Rijke. Large-scale validation of counterfactual learning methods: A test-bed. 2016. URL <http://arxiv.org/abs/1612.00367>.
- [21] L. Li, W. Chu, J. Langford, T. Moon, and X. Wang. An unbiased offline evaluation of contextual bandit algorithms with generalized linear models. In *Proceedings of the Workshop on On-line Trading of Exploration and Exploitation 2*, 2012.
- [22] D. C. Liu and J. Nocedal. On the limited memory bfgs method for large scale optimization. *Mathematical programming*, 45(1-3):503–528, 1989.
- [23] A. Maurer and M. Pontil. Empirical bernstein bounds and sample variance penalization. In *Conference on Learning Theory (COLT)*, 2009.
- [24] T. Nedelec, N. L. Roux, and V. Perchet. A comparative study of counterfactual estimators. *arXiv preprint arXiv:1704.00773*, 2017.
- [25] A. B. Owen. *Monte Carlo theory, methods and examples*. 2013.
- [26] C. Paquette, H. Lin, D. Drusvyatskiy, J. Mairal, and Z. Harchaoui. Catalyst for gradient-based nonconvex optimization. In *International Conference on Artificial Intelligence and Statistics (AISTATS)*, 2018.
- [27] J. M. Robins and A. Rotnitzky. Semiparametric efficiency in multivariate regression models with missing data. *Journal of the American Statistical Association*, 90(429):122–129, 1995.
- [28] R. T. Rockafellar. Monotone operators and the proximal point algorithm. *SIAM journal on control and optimization*, 14(5):877–898, 1976.
- [29] J. Schulman, F. Wolski, P. Dhariwal, A. Radford, and O. Klimov. Proximal policy optimization algorithms. *arXiv preprint arXiv:1707.06347*, 2017.
- [30] Y. Su, L. Wang, M. Santacatterina, and T. Joachims. Cab: Continuous adaptive blending for policy evaluation and learning. In *International Conference on Machine Learning*, pages 6005–6014, 2019.
- [31] R. S. Sutton, D. A. McAllester, S. P. Singh, and Y. Mansour. Policy gradient methods for reinforcement learning with function approximation. In *Advances in Neural Information Processing Systems (NIPS)*, 2000.
- [32] A. Swaminathan and T. Joachims. Counterfactual risk minimization: Learning from logged bandit feedback. In *International Conference on Machine Learning (ICML)*, 2015.

- [33] A. Swaminathan and T. Joachims. The self-normalized estimator for counterfactual learning. In *Advances in Neural Information Processing Systems (NIPS)*. 2015.
- [34] Y.-X. Wang, A. Agarwal, and M. Dudík. Optimal and adaptive off-policy evaluation in contextual bandits. In *International Conference on Machine Learning (ICML)*, 2017.
- [35] C. K. Williams and M. Seeger. Using the nystrom method to speed up kernel machines. In *Adv. Neural Information Processing Systems (NIPS)*, 2001.
- [36] R. J. Williams. Simple statistical gradient-following algorithms for connectionist reinforcement learning. *Machine learning*, 8(3-4):229–256, 1992.

Appendix

This appendix is organized as follows: in Appendix 8, we present a review of off-policy estimators, then in Appendix 9, we present discussions and toy experiments to motivate the need for clipping strategies on real datasets. Next, we provide motivations in Appendix 10 for the offline evaluation protocol with experiments justifying the need for appropriate diagnostics and statistical testing for importance sampling. Then, Appendix 11 is devoted to experimental details that were omitted from the main paper for space limitation reasons, and which are important for reproducing our results (see also the code provided with the submission). In Appendix 12, we present additional experimental results to those in the main paper. Finally, we provide proof for the Proposition 4.1 in Appendix 13.

8 Review of Off-policy Estimators

In Equation (3), the counterfactual approach tackles the distribution mismatch between the logging policy $\pi_0(\cdot|x)$ and a policy π in Π via importance sampling and performs inverse propensity scoring (IPS, [13]). However, the empirical (IPS) estimator has large variance and may overfit negative feedback values y_i for samples that are unlikely under π_0 (see motivation for clipped estimators in 9.2), resulting in higher variances. Clipping the importance sampling weights in Eq. (9) as Bottou et al. [8] mitigates this problem, leading to a new clipped (cIPS) estimator:

$$\hat{L}_{\text{cIPS}}^M(\pi) = \frac{1}{n} \sum_{i=1}^n y_i \min \left\{ \frac{\pi(a_i|x_i)}{\pi_{0,i}}, M \right\}. \quad (9)$$

Smaller values of M reduce the variance of $\hat{L}^M(\pi)$ but induce a larger bias. Swaminathan and Joachims [32] also propose adding an empirical variance penalty term controlled by a factor λ to the empirical risk $\hat{L}^M(\pi)$, leading to a regularized objective with hyperparameters M and λ for clipping and variance penalization, respectively.

Swaminathan and Joachims [33] also introduce a regularization mechanism for tackling the so-called *propensity overfitting* issue, occurring with rich policy classes, where the method would focus only on maximizing (resp. minimizing) the sum of ratios $\pi(a_i|x_i)/\pi_{0,i}$ for negative (resp. positive) losses. This effect is corrected through the following *self-normalized importance sampling* (SNIPS) estimator (see also [25]), which is equivariant to additive shifts in loss values:

$$\hat{L}_{\text{SNIPS}}(\pi) = \frac{\sum_{i=1}^n y_i w_i^\pi}{\sum_{i=1}^n w_i^\pi}, \quad \text{with } w_i^\pi = \frac{\pi(a_i|x_i)}{\pi_{0,i}}. \quad (10)$$

Direct methods (DM) fit the loss values over contexts and actions in observed data with an estimator $\hat{\eta}(x, a)$, for instance by using ridge regression to fit $y_i \approx \hat{\eta}(x_i, a_i)$, and to then use the deterministic greedy policy $\hat{\pi}_{\text{DM}}(x) = \arg \min_a \hat{\eta}(x, a)$. These may suffer from large bias since it focuses on estimating losses mainly near actions that appear in the logged data but have the benefit of avoiding the high-variance problems of IPS-based methods. While such greedy deterministic policies may be sufficient for exploitation, stochastic policies may be needed in some situations, for instance when one wants to still encourage some exploration in a future round of data logs, perhaps for non-stationarity issues. Using a stochastic policy also allows us to obtain more accurate off-policy estimates when performing cross-validation on logged data. Then, we consider a stochastic version of the direct method by adding some Gaussian noise with variance σ^2 :

$$\hat{\pi}_{\text{SDM}}(\cdot|x) = \mathcal{N}(\hat{\pi}_{\text{DM}}(x), \sigma^2), \quad (11)$$

In the context of offline evaluation on bandit data, such a smoothing procedure may also be seen as a form of kernel smoothing for better estimation [17].

Additionally, such direct loss estimators can be effective when few samples are available, and may be combined with IPS estimators in the so-called doubly robust estimator (DR, see, e.g. [10]). This approach consists of correcting the bias of the DM estimator by applying IPS to the residuals $y_i - \hat{\eta}(x_i, a_i)$, thus using $\hat{\eta}$ as a control variate to decrease the variance of IPS.

9 Motivation for Clipped Estimators

In this section we provide an illustration of the logarithmic soft clipping and a motivation example for clipping strategies in counterfactual systems.

9.1 Soft clipping details

Soft clipping strategies are useful for learning on real-life datasets with outliers and to avoid variance in IPS estimates. The lower the clipping parameter is, the more biased the estimate is, but the higher it is the more likely it is to overfit, particularly for low propensities. We illustrate in Fig. 5 the expression of the logarithmic clipping:

$$\zeta(w_i, M) = \begin{cases} w_i & \text{if } w_i \leq M \\ \alpha(M) \log(w_i + \alpha(M) - M) & \text{otherwise,} \end{cases} \quad (12)$$

where $\alpha(M)$ is such that $\alpha(M) \log(\alpha(M)) = M$.

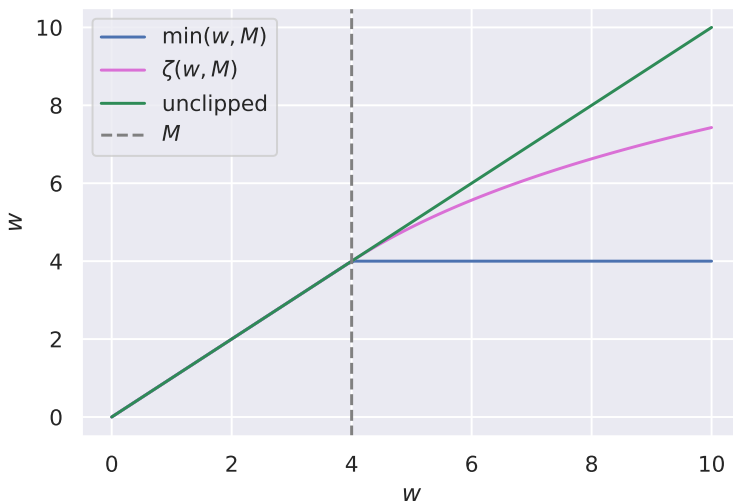


Figure 5: Soft Clipping of importance sampling weight w .

9.2 A Toy Example for Soft Clipping

In Figure 6 we provide an example of unbounded variance and loss overfitting problem.

We recall the data generation: a hidden group label g in \mathcal{G} is drawn, and influences the associated context distribution x and of an unobserved potential p in \mathbb{R} , according to a joint conditional distribution $P_{X,P|G}$. The observed reward r is then a function of the context x , action a , and potential p . Here, we design one outlier (big red dark dot on Figure 5 left). This point has a noisy reward r , higher than neighbors, and a potential p high as its neighbors have a low potential. We artificially added a noise in the reward function f that can be written as:

$$r = f(a, x, p) + \epsilon, \quad \epsilon \sim \mathcal{N}(0, 1)$$

As explained in Section 6.1, the reward function is a linear function, with its maximum localized at the point $x = p(x)$, i.e. at the potential sampled. The observability of the potential p is only through this reward function f . Hereafter, we compare the optimal policy computed, using different type of estimators.

The task is to predict the high potentials (red circles) and low potentials (blue circles) in the ground truth data (left). Unfortunately, a rare event sample with high potential is put in the low potential cluster (big dark red dot). The action taken by the logging policy is low while the reward is high: this sample is an

outlier because it has a high reward while being a high potential that has been predicted with a low action. The resulting unclipped estimator is biased and overfits this high reward/low propensity sample. The rewards of the points around this outlier are low as the diameter of the points in the middle figure show. Inversely, clipped estimator with soft-clipping succeeds to learn the potential distributions, does not overfit the outlier, and has larger rewards than the clipping policies as the diameter of the points show.

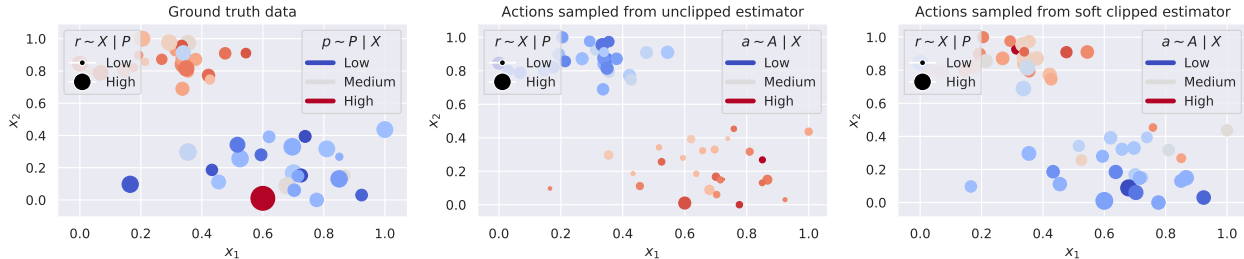


Figure 6: **Unbounded variance and loss overfitting.** Unlikely ($\pi_{0,i} \approx 0$) sample $(x_1, x_2) = (0.6, 0)$ with high reward r (left) results in larger variance and loss overfitting for the unclipped estimator (middle) unlike clipped estimator (right).

10 Motivation for Offline Evaluation Protocol

In this part we demonstrate the offline/online correlation of the estimator we use for real-world systems and for validation of our methods even in synthetic and semi-synthetic setups. We provide further explanations of the necessity of importance sampling diagnostics and we perform experiments to empirically assess the rate of false discoveries of our protocol.

10.1 Correlation of Self-Normalized Importance Sampling with Online Rewards

We show in Figures 7,9,8 comparisons of IPS and SNIPS against an on-policy estimate of the reward for policies obtained from our experiments for linear and non-linear contextual modellings on the synthetic datasets, where policies can be directly evaluated online. Each point represents an experiment for a model and a hyperparameter combination. We measure the R^2 score to assess the quality of the estimation, and find that the SNIPS estimator is indeed more robust and gives a better fit to the on-policy estimate. Note also that overall the IPS estimates illustrate severe variance compared to their SNIPS estimate. While SNIPS indeed reduces the variance of the estimate, the bias it introduces does not deteriorate too much its (positive) correlation with the online evaluation.

These figures further justify the choice of the self-normalized estimator SNIPS [33] for offline evaluation and validation to estimate the reward on held-out logged bandit data. The SNIPS estimator is indeed more robust to the reward distribution thanks to its equivariance property to additive shifts and does not require hyperparameter tuning.

10.2 Experimental validation of the protocol

While the goal of counterfactual learning is to find a policy $\hat{\pi}$ which is as close a possible to the optimal policy π^* , importance sampling estimates are somehow limited in practice when the optimal policy π^* is too "far" from the logging policy π_0 . Therefore for real-world applications one may focus on improving over the logging policy to deploy a policy in production systems in order to progressively collect new data. Thus, it is required to derive level of confidences when estimating the risk of an empirically optimized policy in order to verify the condition $\pi \succ \pi_0$ which we define as $L(\pi) \leq L(\pi_0)$.

We empirically evaluate our offline evaluation protocol on a toy setting where we compare the predictions made with the IPS offline metric as well as the SNIPS offline metric. Offline evaluations of policies $\hat{\pi}$ illustrated

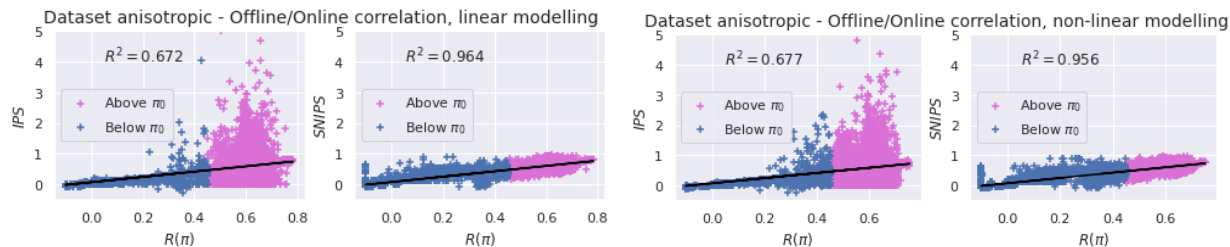


Figure 7: **Correlation between offline and online estimates on Anisotropic synthetic data.** Linear (left) and non-linear (right) contextual modellings. Ideal fit would be $y = x$.

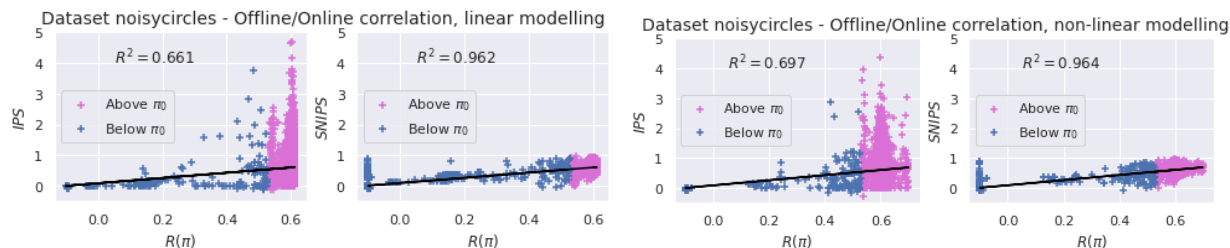


Figure 8: **Correlation between offline and online estimates on NoisyCircles synthetic data.** Linear (left) and non-linear (right) contextual modellings. Ideal fit would be $y = x$.

in Fig. (10) are estimated from logged data $(x_i, a_i, y_i, \pi_0)_{i=1\dots n}$ where $a_i \sim \pi_0(\cdot|x_i)$ and where rewards $-y$ would be optimal for the oracle policy π^* .

Specifically, we evaluate the quality/efficiency of offline estimates for policies (i) "close" to the logging policy and (ii) "close" to the oracle optimal policy. For both setups (i) and (ii), we compare the number of false positives and false negatives of the two offline protocols for 2000 initializations and also show histograms of the differences between online and offline boundary decisions for $\hat{\pi} \succ \pi_0$. Specifically, we use the upper bound of a two-sided, $1 - \delta$ confidence interval for the difference in risks performance ϵ_π (compared to π_0) i.e. $\epsilon_\pi = [\hat{L}_{\text{SNIPS}}(\pi) - \hat{L}(\pi_0)]_{1-\delta/2}$ as referred in Algorithm 1. This quantity shall be adjusted in case of multiple testing. More precisely, if one evaluates an algorithm with k random seeds and using a parameter grid of size l , we suggest to adjust the δ threshold for $k \times l$ tests (e.g. Bonferroni adjustment [7], Benjamini-Hochberg procedure [5], ...). Alternatively, one may choose hyper-parameters and seed by cross-validation on the train set (including any multiple testing procedure) and perform the significance test only once on the test set with the latter policy. This specific evaluation procedure is let for future work.

10.2.1 Perturbation to the logging policy π_0

Knowing the closed form of the logging policy π_0 and its parameters, we add Gaussian noise to the parameters of π_0 and use the offline evaluation protocol to discard solutions with importance sampling diagnostics (effective sample sizes < 0.01) and estimate confidence intervals with bootstrap procedures on the test set.

We observe that the SNIPS estimate has fewer false positives and false negatives, as shown in Table 3. Histograms of boundary decisions $\epsilon_\pi = [\hat{L}_{\text{SNIPS}}(\pi) - \hat{L}(\pi_0)]_{1-\delta/2}$ illustrated in Fig. 11 show that the IPS estimate underestimates the value of the reward with regard to the online estimate and has a lot of variance, unlike the SNIPS estimates which exhibits less variance and seems centered around the online estimate.

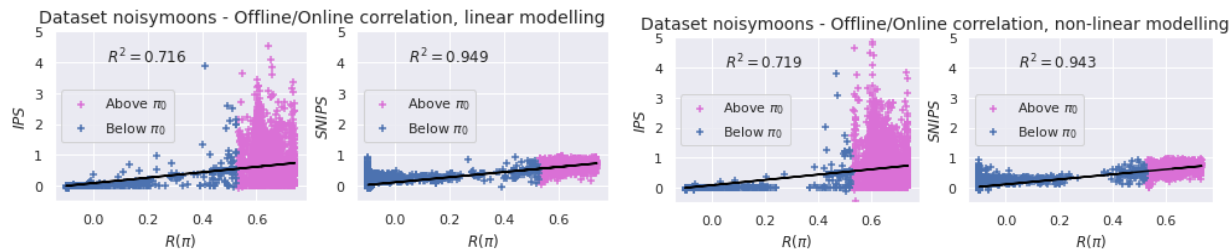


Figure 9: **Correlation between offline and online estimates on NoisyMoons synthetic data.** Linear (left) and non-linear (right) contextual modellings. Ideal fit would be $y = x$.

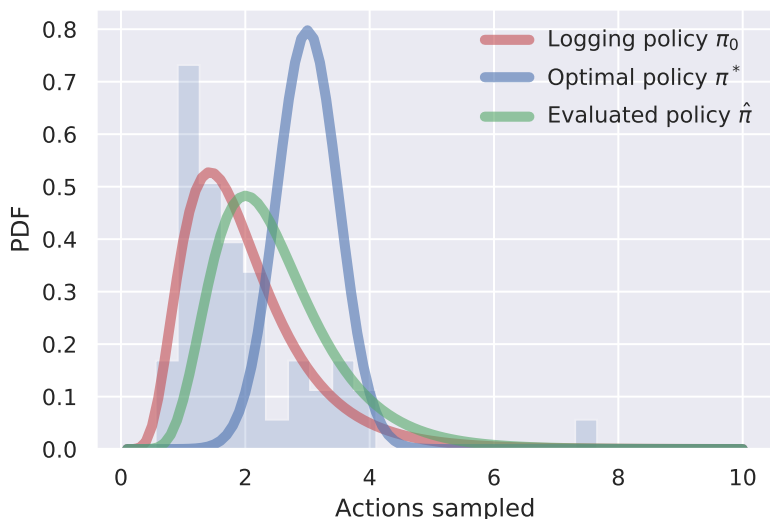


Figure 10: **Offline evaluation protocol.**

10.2.2 Perturbation to the oracle policy π^*

Knowing the closed form of the oracle policy π^* and its parameters, we add Gaussian noise to its parameters and use the same protocol as before. This setup is "harder" than the previous one since importance sampling is more likely to fail when the evaluated policy is too "far" from the logging policy.

We observe that the SNIPS estimate has a drastically lower number of false negatives than the IPS estimate, though it has more false positives as shown in Table 4. Once again as illustrated in Figure 12, the IPS estimate underestimates the value of the reward with regard to the online estimate and large variance which may explain why IPS does not have false positives where the evaluated policy is far from the logging policy.

10.2.3 Influence of the effective sample size criteria in the evaluation protocol

In Fig. 13 we show how the effective sample size (ESS) threshold influences the performance of the offline evaluation protocol for the two previously discussed setups where we consider evaluations of (i) perturbations of the logging policy and (ii) perturbations of the optimal policy in synthetic setups. We compute precision, recall and F1 scores for each threshold values between 0 and 1. For low threshold values where no policies are filtered, precision, recall and F1 scores remain unchanged but performance increases at a certain point but then drops because of the protocol generating more false negatives. ESS criteria is even more relevant for

Table 3: **Comparison of false positives and false negatives:** Perturbation to the logging policy π_0

	Offline Protocol	IPS		SNIPS	
		$\hat{\pi} \succeq \pi_0$	Fail	$\hat{\pi} \succeq \pi_0$	Fail
"Truth"	$\hat{\pi} \succeq \pi_0$	1282	24	1296	10
	Fail	19	675	0	694

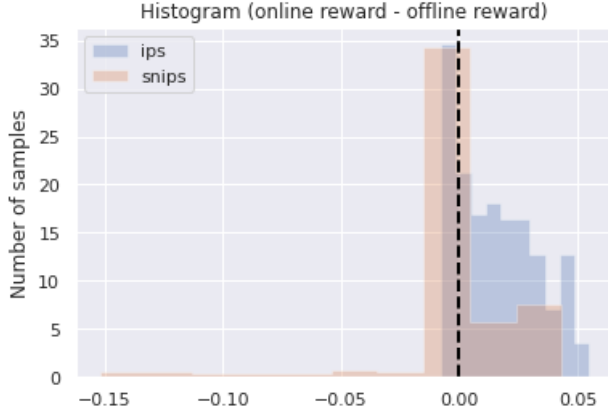


Figure 11: **Histogram of differences between online reward and offline lower confidence bound.** Perturbation to the logging policy π_0

policies which are "far" from the logging policy as shown in the right part of Fig. 13 and explained in next subsection on importance sampling diagnostics in what-if simulations 10.3.

10.3 Importance Sampling Diagnostics in What-If simulations

Importance sampling estimators rely on weighted observations to address the distribution mismatch for offline evaluation, which may cause large variance of the estimator. Notably, when the evaluated policy differs too much from the logging policy, many importance weights are large and the estimator is inaccurate. We provide here a motivating example to illustrate the effect of importance sampling diagnostics in a simple scenario.

When evaluating with SNIPS, we may consider an "effective sample size" quantity given in terms of the importance weights $w_i = \pi(a_i|x_i)/\pi_0(a_i|x_i)$ by $n_e = (\sum_{i=1}^n w_i)^2 / \sum_{i=1}^n w_i^2$. When this quantity is much smaller than the sample size n , this indicates that only few of the examples contribute to the estimate, so that the obtained value is likely a poor estimate. Apart from that, we note also that IPS weights have an expectation of 1 when summed over the logging policy distribution (that is $\mathbb{E}_{(x,a) \sim \pi_0} [\pi(a|x)/\pi_0(a|x)] = 1$). Therefore, another sanity check, which is valid for any estimator, is to look for the empirical mean $1/n \sum_{i=1}^n \pi(a_i|x_i)/\pi_{0,i}$ and compare its deviation to 1. In the example below, we illustrate three diagnostics: (i) the one based on effective sample size described in Section 5; (ii) confidence intervals, and (iii) empirical mean of IPS weights. The three of them coincide and allow us to remove test estimates when the diagnostics fail.

Example 10.1. *What-if simulation:* For x in \mathbb{R}^d , let $\max(x) = \max_{1 \leq j \leq d} x_j$; we wish to estimate $\mathbb{E}(\max(X))$ for X i.i.d $\sim \pi_\mu = \mathcal{N}(\mu, \sigma)$ where samples are drawn from a logging policy $\pi_0 = \log \mathcal{N}(\lambda_0, \sigma_0)$ ($d = 3$, $(\lambda_0, \sigma_0) = (1, 1/2)$) and analyze parameters μ around the mode of the logging policy μ_{π_0} with fixed variance $\sigma = 1/2$. In this parametrized policy example, we see in Fig. 14 that $n_e/n \ll 1$, confidence interval range increases and $\sum_{i=1}^n \frac{\pi(a_i|x_i)}{\pi_{0,i}} \neq 1$ when the parameter μ of the policy being evaluated is far away from the logging policy mode μ_{λ_0} .

Note that in this example, the parameterized distribution that is learned (multivariate Gaussian) is not the same as the parameterized distribution of the logging policy (multivariate Lognormal) which skewness

Table 4: Comparison of false positives and false negatives: perturbations to the optimal policy π^*

	Offline Protocol	IPS		SNIPS	
		$\hat{\pi} \succeq \pi_0$	Fail	$\hat{\pi} \succeq \pi_0$	Fail
"Truth"	$\hat{\pi} \succeq \pi_0$	1565	67	1631	1
	Fail	0	368	6	362

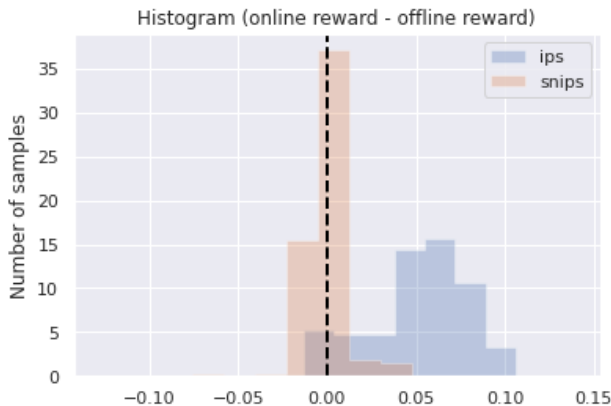


Figure 12: Histogram of differences between online reward and offline lower confidence bound. Perturbation to the optimal policy π^*

may explain the asymmetry of the plots. This points out another practical problem: even though different parametrization of policies is theoretically possible, the probability density masses overlap is in practice what is most important to ensure successful importance sampling. This observation is of utmost interest for real-life applications where the initialization of a policy to be learned needs to be "close" to the logging policy; otherwise importance sampling may fail from the very first iteration of an optimization in learning problems.

11 Details on the Experiment Setup and Reproducibility

In this section we give additional details on synthetic and semi-synthetic datasets, we provide details on the evaluation methodology and information for experiment reproducibility.

11.1 Synthetic and Semi-Synthetic setups

Synthetic setups The three generated synthetic datasets called “noisymoons, noisycircles, and anisotropic”, are illustrated in Figure 15, with two-dimensional contexts $\mathcal{X} = \mathbb{R}^2$ and 2 or 3 groups.

As many real-world applications feature a reward function that increases first with the action, then plateaus and finally drops, we have chosen a piecewise linear function as shown in Fig. 16 that mimics reward buckets over the CoCoA dataset presented in Section 5.

Semi-synthetic medical setup The semi-synthetic loss inputs prescriptions from medical experts to obtain $y(a, x) = \max(|a - t^*| - 0.1t^*, 0)$. The logging policy π_0 samples actions $a \sim \pi_0$ contextually to a patient’s BMI z -score $Z_{BMI} = \frac{x_{BMI} - \mu_{BMI}}{\sigma_{BMI}}$ and can be analytically written with i.i.d noise $e \sim \mathcal{N}(0, 1)$, moments of the therapeutic dose distribution μ_T^*, σ_T^* such that $a = \mu_T^* + \sigma_T^* \sqrt{\theta} Z_{BMI} + \sigma_T^* \sqrt{1 - \theta} e$ ($\theta = 0.5$ in the setup of [17]). The logging probability density function thus is a continuous density of a standard normal distribution over the quantity $\frac{a - \mu_T^* + \sigma_T^* \sqrt{\theta} Z_{BMI}}{\sigma_T^* \sqrt{1 - \theta}}$.

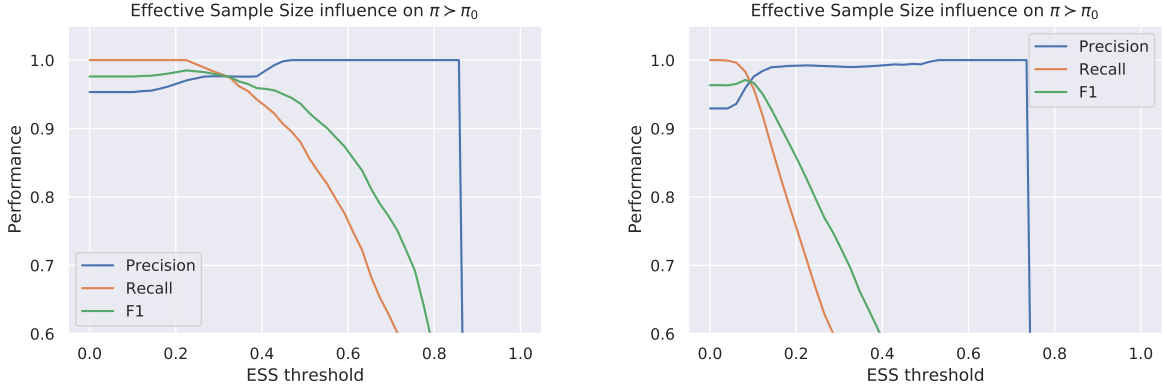


Figure 13: **Precision, recall and F1 score varying with the ESS threshold.** Perturbation of the logging policy (left) and optimal policy (right).

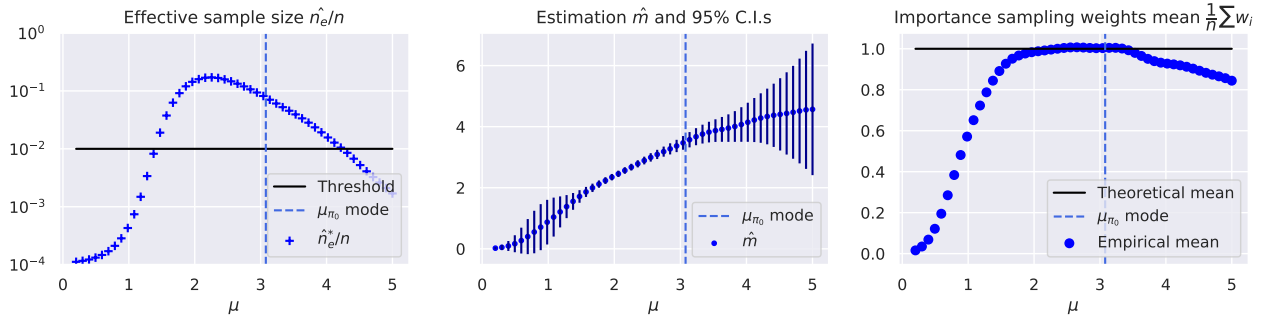


Figure 14: **Importance sampling diagnostics.** Ideal importance sampling: i) effective sample n_e/n close to 1, ii) low confidence intervals (C.I.s) for \hat{m} , iii) empirical mean $\frac{1}{n} \sum_i w_i$ close to 1. Note that when μ differs too much from μ_{π_0} , importance sampling fails.

11.2 Evaluation methodology.

For synthetic datasets, we generate training, validation, and test sets of size 10000 each. For the CoCoA dataset, we consider a 50%-25%-25% training-validation-test sets. We then run each method with 5 different random initializations such that the initial policy is close to the logging policy. Hyperparameters are selected on a validation set with logged bandit feedback, by using an offline SNIPS estimate of the obtained policies, while discarding solutions deemed unsafe with the importance sampling diagnostic. For estimating the final test performance and confidence intervals on synthetic datasets, we use an online estimate by leveraging the known reward function and taking a Monte Carlo average with 100 action samples per context: this accounts for the randomness of the policy itself over given fixed samples. For offline estimates we leverage the randomness across samples to build confidence intervals: we use a 100-fold bootstrap and take percentiles of the distribution of rewards as given in Algo 1. For the CoCoA dataset, we use the latter methodology in our reported test metrics.

11.3 Reproducibility

We provide code for reproducibility and all experiments were run on a cpu cluster, each node consisting on 24 CPU cores (2 x Intel(R) Xeon(R) Gold 6146 CPU@ 3.20GHz), with 500Go of RAM.

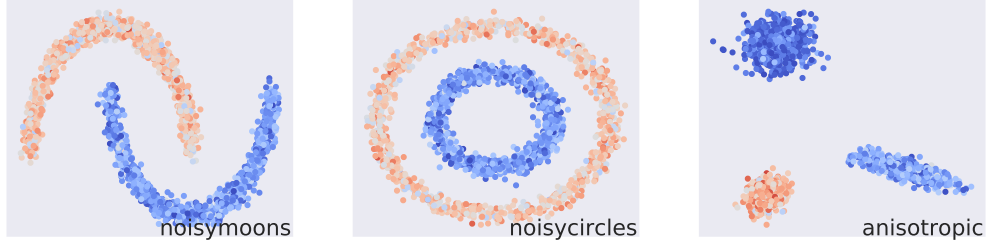


Figure 15: **Contexts (points in \mathbb{R}^2), and potentials represented by a color map for the synthetic datasets.** Learned policies should vary with the context to adapt to the underlying potentials.

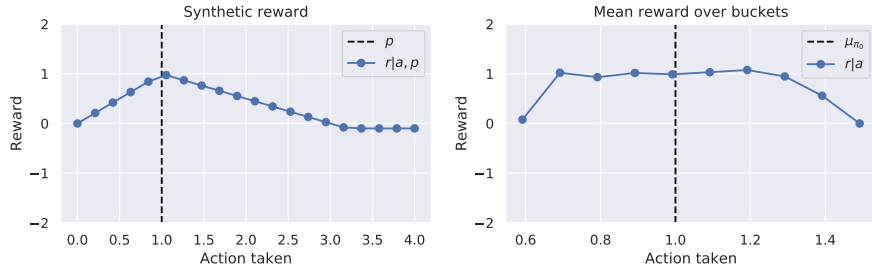


Figure 16: **Synthetic reward engineering.** The synthetic reward (left) is inspired from real-dataset reward buckets (right).

Policy parametrization. In our experiments, we consider two forms of parametrizations: (i) a lognormal distribution with $\theta = (\theta_\mu, \sigma)$, $\pi_{(\mu, \sigma)} = \log \mathcal{N}(m, s)$ with $s = \sqrt{\log(\sigma^2/\mu^2 + 1)}$; $m = \log(\mu) - s^2/2$, so that $\mathbb{E}_{a \sim \pi_{(\mu, \sigma)}}[a] = \mu$ and $\text{Var}_{a \sim \pi_{(\mu, \sigma)}}[a] = \sigma^2$; (ii) a normal distribution $\pi_{(\mu, \sigma)} = \mathcal{N}(\mu, \sigma)$. In both cases, the mean μ may depend on the context (see Section 4), while the standard deviation σ is a learned constant. We add a positivity constraint for σ and add an entropy regularization term to the objective in order to encourage exploratory policies and avoid degenerate solutions.

Models. For our experiments involving anchor points, we took $m = 10$ anchor points on the synthetic and semi-synthetic dataset and $m = 3$ for the CoCoA dataset. For parametrized distributions, we experimented both with normal and lognormal distributions on all datasets, and different baseline parameterizations including constant, linear and quadratic. Some of our experiments on low-dimensional datasets also consider a stratified piece-wise contextual parameterization, which partitions the space by bucketizing each feature by taking K quantiles, with $K = 4$, and taking the cross product of these partitions for each feature.

Hyperparameters. In Table 5 we show the hyperparameters considered to run the experiments to reproduce all the results. Note that the grid of hyperparameters is larger for synthetic data.

Table 5: Table of hyperparameters for the Synthetic and CoCoA datasets

	Synthetic	Warfarin	CoCoA
Variance reg. λ	{0., 0.001, 0.01, 0.1, 1, 10, 100}	{0.00010.0010.010.1}	{0., 0.001, 0.1}
Clipping M	{1, 1.7, 2.8, 4.6, 7.7, 12.9, 21.5, 35.9, 59.9, 100.0}	{1, 2.1, 4.5, 9.5, 20}	{1, 2.1, 4.5, 9.5, 10, 20, 100}
Prox. κ	{0.001, 0.01, 0.1, 1}	{0.001, 0.01, 0.1}	{0.001, 0.01, 0.1}
Reg. param. C	{0.00001, 0.0001, 0.001, 0.01, 0.1}	{0.00001, 0.0001, 0.001, 0.01, 0.1}	{0.00001, 0.0001, 0.001, 0.01, 0.1}
Reg. entropy ϵ	{0.0001, 0.01, 1.}	{0.0001, 0.01}	{0.0001, 0.01}
Softmax γ	{1, 10, 100}	{1, 10}	{0.1, 0.5, 1}

12 Additional Results and Additional Evaluation Metrics

In this section we provided additional results on both contextual modeling and optimization driven approaches of CRM.

12.1 Continuous vs Discrete strategies in continuous-action space

We provide in Figure 17 additional plots for the continuous vs discrete strategies for the synthetic setups described in Section 6.1.

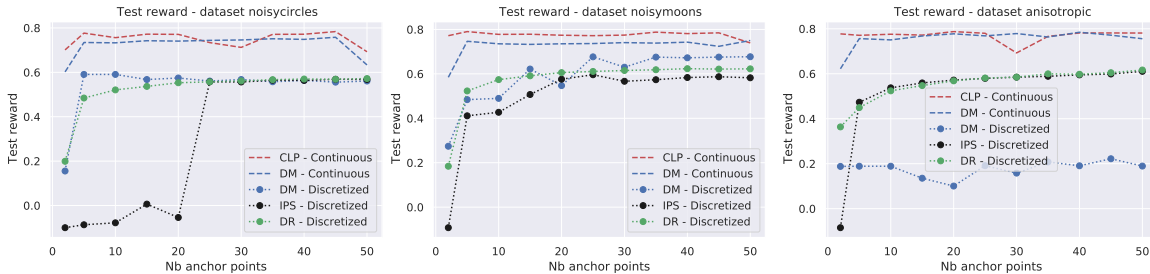


Figure 17: **Continuous vs discrete.** Test rewards for CLP and (stochastic) direct method (DM) with Nyström parameterization, versus a discrete approach, with varying numbers of anchor points. We add a minimal amount of noise to the deterministic DM in order to pass the n_{eff} validation criterion.

12.2 Contextual Modeling Comparisons

We show additional comparisons of contextual models for stochastic policies for other estimators in Table 6. On the synthetic datasets, it is easy to beat the logging policy with high level of confidence and with the importance sampling diagnostics. For the CoCoA dataset, we build offline statistical confidence interval with bootstrap percentiles as described in Algo 1.

For the CoCoA dataset, it is highly difficult to obtain policies with high offline estimates that verify the importance sampling diagnostics with bootstrap confidence intervals that do not intersect with the logging policy, but note that a significant improvement is achieved for the CLP model with the SNIPS estimator (see the asterisk in Table 6, which indicates a significant improvement over the logging policy according to our protocol in Algorithm 1). We also note that the SNIPS estimator in CRM achieves the best performances for both the semi-synthetic and CoCoA datasets, while for the synthetic datasets, IPS and clipped IPS seem to lead to better policies.

12.3 Optimization Driven Approaches of CRM

In this part we provide additional results on optimization driven approaches of CRM for the Noisycircles, Anisotropic, Warfarin and CoCoA datasets.

Both Noisycircles and Anisotropic datasets in Figure 18 show the improvements in test reward and in training objective of our optimization-driven strategies, namely the soft-clipping estimator and the use of the proximal point algorithm. Overall we see that for most configurations, the proximal point method better optimizes the objective function and provides better test performances, while the soft-clipping estimator performs better than its hard-clipping variant, which may be attributed to the better optimization properties. For semi-synthetic Warfarin and real-world CoCoA datasets in Figure 18 we also show the improvements in test reward and in training objective of our optimization-driven strategies. More particularly we demonstrate the effectiveness of proximal point methods on the Warfarin dataset where most proximal configurations perform better than the base algorithm. Moreover, soft-clipping strategies perform better than its hard-clipping

Table 6: **Comparison of policy parameterizations on all datasets for different CRM estimators.** Test rewards are shown with one standard deviation estimated across contexts. This is a more comprehensive version of Table 2.

		Noisycircles	NoisyMoons	Anisotropic	Warfarin	CoCoA
Logging policy π_0		0.5301	0.5301	0.4533	-13.3769	11.34
IPS	constant	0.6114 ± 0.0001	0.6114 ± 0.0001	0.6018 ± 0.0001	-10.066 ± 0.003	11.35 ± 0.01
	linear	0.6115 ± 0.0001	0.7329 ± 0.0001	0.7465 ± 0.0007	-10.295 ± 0.009	11.37 ± 0.02
	non-linear	0.6943 ± 0.0001	0.7137 ± 0.0001	0.7301 ± 0.0010	-	10.17 ± 0.12
	clp	0.7663 ± 0.0003	0.7432 ± 0.0004	0.8047 ± 0.0002	-11.392 ± 0.003	11.35 ± 0.03
cIPS	constant	0.6116 ± 0.0001	0.6116 ± 0.0001	0.6026 ± 0.0001	-10.064 ± 0.003	11.36 ± 0.13
	linear	0.6115 ± 0.0001	0.7337 ± 0.0001	0.7465 ± 0.0007	-9.2159 ± 0.030	11.35 ± 0.02
	non-linear	0.6927 ± 0.0001	0.7287 ± 0.0001	0.7483 ± 0.0003	-	10.17 ± 0.08
	clp	0.7925 ± 0.0006	0.7940 ± 0.0004	0.8011 ± 0.0002	-10.007 ± 0.003	11.34 ± 0.09
scIPS	constant	0.6115 ± 0.0000	0.6116 ± 0.0000	0.6026 ± 0.0000	-10.050 ± 0.003	11.36 ± 0.13
	linear	0.6113 ± 0.0001	0.7326 ± 0.0001	0.7638 ± 0.0005	-10.291 ± 0.004	8.00 ± 0.72
	non-linear	0.6959 ± 0.0001	0.7281 ± 0.0001	0.7448 ± 0.0008	-	8.78 ± 0.51
	clp	0.7674 ± 0.0008	0.7805 ± 0.0004	0.7703 ± 0.0002	-9.988 ± 0.001	11.44* ± 0.10
SNIPS	constant	0.6115 ± 0.0001	0.6115 ± 0.0001	0.5930 ± 0.0001	-8.92 ± 0.0006	11.32 ± 0.13
	linear	0.6115 ± 0.0001	0.7360 ± 0.0001	0.7103 ± 0.0003	-14.158 ± 0.0003	10.34 ± 0.12
	non-linear	0.6969 ± 0.0001	0.7370 ± 0.0001	0.5801 ± 0.0002	-	11.13 ± 0.08
	clp	0.6972 ± 0.0001	0.74091 ± 0.0004	0.7899 ± 0.0002	-8.505 ± 0.007	11.48* ± 0.14

variant on real-world dataset with outliers and noises, which demonstrate the effectiveness of this smooth estimator for real-world setups.

Note also that using the importance sampling diagnostics is crucial to ensure an estimator is reliable on the test set. Indeed, when removing the importance sampling diagnostics, experiments show results which are either drastically below or much higher than the logging policy. The importance sampling diagnostics thus helps avert unsuccessful estimates and prevents from overestimating possible solutions. On the CoCoA dataset especially, beating the logging policy with a high level of confidence and makes offline estimation on real-life bandit feedback datasets a fundamental problem.

13 Generalization Bound for the Soft-Clipping Estimator \hat{R}_{scIPS}^M (proof of Proposition 4.1)

In this section, we derive a simple generalization bound on the risk for the soft-clipping estimator with empirical variance regularization, following Maurer and Pontil [23], Swaminathan and Joachims [32]. Recall the estimator

$$\hat{R}_{\text{scIPS}}^M(\pi) = \frac{1}{n} \sum_{i=1}^n \nu_i(\pi), \quad \text{with} \quad \nu_i(\pi) = y_i \zeta \left(\frac{\pi(a_i|x_i)}{\pi_0(a_i|x_i)}, M \right),$$

and the empirical variance which is used for regularization:

$$\hat{V}(\pi) = \frac{1}{n-1} \sum_{i=1}^n (\nu_i(\pi) - \bar{\nu}(\pi))^2, \quad \text{with} \quad \bar{\nu}(\pi) = \frac{1}{n} \sum_{i=1}^n \nu_i(\pi).$$

We assume that losses $y_i \in [-1, 0]$ almost surely, as in [32], and make the additional assumption that the importance weights $\pi(a_i|x_i)/\pi_0(a_i|x_i)$ are upper bounded by a constant W almost surely for all $\pi \in \Pi$. This is verified, for instance, if all policies have a given compact support (e.g., actions are constrained to belong to a given interval) and π_0 puts mass everywhere in this support.

We state the bound for a finite policy class for simplicity, but we remark below that it extends to infinite policy classes through covering numbers. Note that while the bound requires importance weights bounded by a constant W , the bound only scales logarithmically with W when $W \gg M$.

Proposition 13.1 (Generalization bound for finite policy class Π). *Assume losses in $[-1, 0]$ and importance weights bounded by W . With probability $1 - \delta$, we have, for all $\pi \in \Pi$,*

$$R(\pi) \leq \hat{R}_{scIPs}^M(\pi) + \sqrt{\frac{2\hat{V}(\pi) \log(2|\Pi|/\delta)}{n}} + S \frac{7 \log(2|\Pi|/\delta)}{3(n-1)}, \quad (13)$$

where $S = \zeta(W, M) = O(\log W)$.

Proof. Let

$$f_i(\pi) = 1 + \frac{y_i}{S} \zeta \left(\frac{\pi(a_i|x_i)}{\pi_0(a_i|x_i)}, M \right).$$

We have $f_i(\pi) \in [0, 1]$ and $\mathbb{E}_{(x_i, a_i, y_i) \sim \mathcal{D}_{\pi_0}}[f_i(\pi)] = 1 + R^M(\pi)/S$, with

$$R^M(\pi) = \mathbb{E}_{(x, a, y) \sim \mathcal{D}_{\pi_0}} \left[y \zeta \left(\frac{\pi(a|x)}{\pi_0(a|x)}, M \right) \right].$$

We can now apply the concentration bound of Maurer and Pontil [23, Corollary 5] to the f_i and rescale appropriately by S to obtain that with probability $1 - \delta$, for all $\pi \in \Pi$,

$$R^M(\pi) \leq \hat{R}_{scIPs}^M(\pi) + \sqrt{\frac{2\hat{V}(\pi) \log(2|\Pi|/\delta)}{n}} + S \frac{7 \log(2|\Pi|/\delta)}{3(n-1)}.$$

We then conclude by noting that $R(\pi) \leq R^M(\pi)$, since $\ell(a) \leq 0$ and $\zeta(w, M) \leq w$ for all w . □

We note that the result above can be extended to infinite policy classes by essentially replacing $|\Pi|$ above with an ℓ_∞ covering number of the set $\{(f_1(\pi), \dots, f_n(\pi)) : \pi \in \Pi\}$, by leveraging Maurer and Pontil [23, Theorem 6] as in [32].

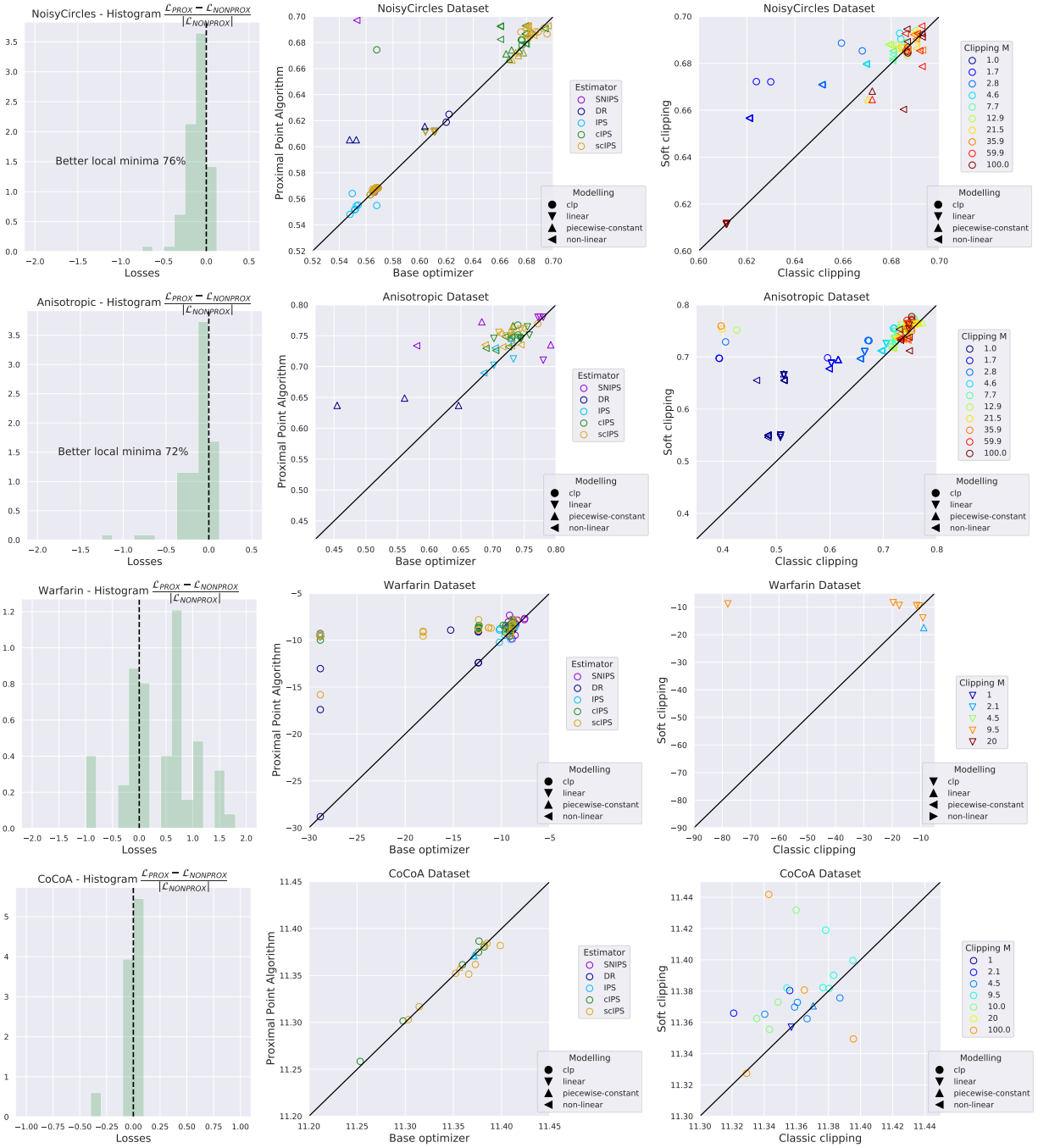


Figure 18: **Optimization-driven approaches** (NoisyCircles, Anisotropic, Warfarin and CoCoA datasets). Relative improvements in the training objective from using the proximal point method (left), comparison of test rewards for proximal point vs the simpler gradient-based method (center), and for soft- vs hard-clipping (right). See also Figure 4 for the NoisyMoons dataset.